Response to Reviewer Comments

July 1, 2021

Author Statement

I thank Dr. Stolzenburg for his time to review this manuscript and his constructive critiques. Below are itemized responses to the referees' comments. In response to the comments, Section 2.3 of the manuscript was significantly expanded. The complete revised section is mentioned in several responses. To avoid repetition, the revised section is reproduced at the end of the document.

Response to Reviewer #2 (Mark Stolzenburg)

Overview

[1] Disclaimer: Other than just some broad principles, this reviewer is not familiar with regularization techniques or the Julia syntax and is therefore ill-equipped to properly review the technical nature of that aspect of this work. Attention is generally focused on other aspects of this paper. Also, the lack of full comprehensive documentation of all the notation used in the equations presented here has frequently hampered a thorough understanding of these equations. However, it is still possible to discern the general meaning of most equations. Equation (10) is a good example of this. The definition of the map() function and the interpretation of the right arrow (→) are not given in the text here. At least the map() function is defined in the Petters (2018) reference. It appears the arrow notation is part of notation for a series or sequence.

[1] Referee

[2] *I apologize for the missing definitions in the draft. These are now included in the revised version.*

[2] *Response*

[3] This manuscript addresses the important issue of automating the processing of tandem DMA data. The idea of inverting data with regularization is sound. However, there are problems with the forward model of calculating system response from a known input distribution. If these issues can be properly addressed, the resulting software package should prove of great utility.

[3] Referee

[4] *I thank Dr. Stolzenburg for his detailed and helpful review comments below. The issue raised regarding the forward model is addressed via a revision of the text and equations. The comments highlighted two assumptions that had no impact on the result, but were important to revise to be as correct as possible.*

[4] *Response*

Major Comments

[5] There appears to be a problem with proper accounting of diffusional losses and broadening of the transfer function, Ω, for DMA2. Eq. (10) in the form of **A** characterizes the transfer through DMA1 while the equation for **O** (line 230) characterizes transfer through DMA2. As noted in Petters [2018], these two expressions are analogous except for the inclusion of T_c in the former and the limitation of the summation to $k = 1$ in the latter. In the DMA, a particle is sized according to its apparent mobility diameter whereas diffusional losses as well as broadening of the transfer function are dependent on the true mobility diameter via particle diffusivity. Given one of these diameters, the particle charge is required to calculate the other and ultimately $T_{size}^{\Lambda,\delta}$. Thus, it is important to sum over all charge states individually to calculate the diffusing transfer through a DMA. As this is not done for the second DMA, the given expression cannot be properly accounting for transfer of multiply charged particles.

[5] Referee

[6] *Thank you for the raising this issue. In fact, the issue affects both the matrix* **A** *and the matrix* **O**. *The version in Petters (2018) and the draft manuscript compute the shape of the transfer function and losses for the mobility diameter corresponding to singly charged particles and then apply the same shape of the transfer function and diffusional loss to the multiply charged particles. The error that is introduced by this assumption/simplification is generally small since the fraction of multiply charged particles is small for sizes when diffusional broadening becomes important, and because the change in the shape of the transfer function/diffusional loss rate between the sizes is small. Nevertheless, there is no need to make this simplification. The formalism is now updated to properly account for the transfer of multiply charged particles.*

[6] *Response*

[7] **Section 2.3 of the manuscript has been revised to include this effect. Since this section includes changes in response to multiple other comments, please see the changed section at the end of this document for details.**

[7] **Revision**

[8] The interpretation of Eq. (11) and its components would be greatly facilitated by an explicit indication of the independent parameters of distribution for the input size distribution $\mathbb{n}^{cn}$. Also, the precise form of $\mathbb{n}^{cn}$ (e.g. dN/dDp, $dN/dlnDp$, or $dN/dlogDp$) is important. The most obvious set of independent particle parameters would be (true) mobility diameter, D_1, and charge, k. However, it appears that $\mathbb{n}^{cn}$ is distributed according to apparent mobility diameter, D_k, and k in order to have the balance of the equation work out. The apparent mobility diameter is then premultiplied by the effective, or apparent, growth factor, $gf_k(z^s, gf_0)$, and then by the ratio of true to apparent mobility diameters, D_1/D_k. However, this ratio is being evaluated at the DMA1 centroid mobility, z^s, but applied to the Z grid after growth. Since this ratio is a function of size, this does not work out. Also, this means that the input distribution to the operator characterizing DMA2 transfer is in terms of true mobility diameter, in contrast to the $\mathbb{n}^{cn}$ input to DMA1 and A. All of this switching back and forth between true and apparent mobility diameter

[8] Referee

seems overly complicated.

[9] *The precise form $\mathbb{n}^{cn}$ is now clarified in the text just above the equation in question. It is a histogram in dN/dlnD units. The "cn" has been dropped based on a later comment. The distribution $\mathbb{n}$ is along the actual mobility diameter. The referee is correct that the way it was formulated in the draft was confusing due to multiple switches between true and apparent mobility diameter. The referee is also correct that the ratio was being evaluated at the DMA1 centroid mobility, z^s, but applied to the Z grid after growth. The assumption was that particles within a charge grouping all behave the same. I changed the equation and the code to make it more intuitive and more correct, i.e. when projecting the physically grown diameter back to mobility space, the correction is applied for each point in the Z grid. The impact on the calculation due to the change is almost imperceptibly. Text has been added to help parsing the equation.*

[9] *Response*

[10]

$$\mathbb{r} = \mathbf{A}\mathbb{n} + \epsilon \tag{12}$$

[10] **Revision**

where $\mathbb{r}$ is the response distribution, $\mathbb{n}$ is the true mobility size distribution, and ϵ is a vector denoting the random error that may be superimposed as a result of measurement uncertainties. Note that by design $\mathbb{n}$ and $\mathbb{r}$ are *SizeDistribution* objects, which represented the distribution as a histogram simultaneously as spectral density units (dN/dlnD) and concentration per bin units. The latter is the raw response function defined as integrated response downstream of the DMA as a function of upstream voltage (or corresponding z^s or corresponding apparent +1 mobility diameter).

The mobility distribution exiting DMA 2 in the humidified tandem DMA is evaluated using the expressions

$$\mathbb{M}_k^{\delta_1} = \Pi_k^{\Lambda,\delta} \cdot \left\{ g_0 \cdot \left[T_{size}^{\Lambda,\delta}(k, z^s) * \mathbb{n} \right] \right\} \tag{13}$$

In Eq. (13), $\mathbb{M}_k^{\delta_1}$ evaluates to the apparent +1 mobility distribution particles that exit the DMA$^{\Lambda,\delta}$ at the nominal setpoint-diameter defined by mobility z^s (or z-star) in DMA 1 and particle charge k. Subscripts are used to differentiate DMA 1 and 2 which possibly have different geometries, flow rates, and grids, e.g. Λ_1, Λ_2 and δ_1, δ_2. $\Pi_k^{\Lambda,\delta}$ is the projection of particles having physical diameter D and carrying k charges onto the apparent +1 mobility grid. It is a function that converts each diameter/charge pair to mobility and interprets the result as apparent +1 mobility diameter. $g_0 = D_{wet}/D_{dry}$ is the true diameter growth factor, D_{dry} is the selected diameter by DMA 1, D_{wet} is the diameter after the humidifier, $T_{size}^{\Lambda,\delta}(k, z^s)$ is as in Eq. (10), and $\mathbb{n}$ is the mobility size distribution upstream of DMA 1.

To help parse Eq. (13), the product $T_{size}^{\Lambda,\delta}(k, z^s) * \mathbb{n}$ evaluates to the transmitted mobility distributions of particles carrying k charges at the set-point mobility z^s in DMA 1. The size distribution is grown by the growth factor g_0. The resulting size distribution is shifted to the apparent +1 mobility diameter using $\Pi_k^{\Lambda,\delta}$. Equation (13) differs from that in Petters [2018] where it was assumed that particles of all charges grow by the same amount. This is incorrect. Particles carrying

more than a single charge alias at a smaller particle size [Gysel et al., 2009, Shen et al., 2021]. The effect is due to the size dependence of the slip-flow correction factor and captured through the function $\Pi_k^{\Lambda,\delta}$. Equation (13) assumes that g_0 applies to all particle sizes.

Minor Comments and Corrections

[11] line 158: Insert a space between "as" and "x". [11] Referee

[12] *Done.* [12] *Response*

[13] line 186: The description of a DMA here is a bit too brief, saying nothing about the flow. Try "Charged particles in a flow between the electrodes are deflected to an exit slit..." [13] Referee

[14] *Thank you for the suggestion. Done.* [14] *Response*

[15] lines 188-189: "The functions ... and tandem DMAs ~~is~~ are well understood ..." [15] Referee

[16] *Done.* [16] *Response*

[17] line 200: "$T \,.\, n$"should be "$T. \,. n$" according to Petters (2018). Presumably T is a vector, but this differs from the notation conventions given in lines 87-88. [17] Referee

[18] *Yes, "$T \,.\, n$"should be "$T. \,. n$" according to Petters (2018). (T is a vector). The original version was developed on julia v0.6 and it allowed me to create the "$T. \,. n$" construct which was desirable to create a consistent treatment of vectors. Once julia updated to 1.x series, it was not longer possible to use this notation and I dropped the extra dot. This difference is now noted in the text.* [18] *Response*

[19] **See updated section 2.3** [19] **Revision**

[20] Eq. (10): Here, $T_{size}^{\Lambda,\delta}$ alone characterizes transfer through the DMA. Evidently the balance of this expression puts this into the required form for later matrix manipulation. Some additional explanation of how this matrix is created from $T_{size}^{\Lambda,\delta}$ would be useful here. And though perhaps only parentheses may be used in programming, the readability of this equation would be greatly improved by alternating "( )" with "[ ]" and "{ }". [20] Referee

[21] *The equation(s) have been updated for readability by alternating "( )" with "[ ]" and "{* [21] *Response*

}". The equation has also been rewritten for clarity by removing julia language specific constructs and giving much more details about the functions used in the text. As pointed out in Petters (2018) "It may not be immediately obvious why the expression ... evaluates to the convolution matrix (or that it evaluates to a matrix at all). A step-by-step explanation is in Notebook S2." The reference to the supplement of the preceding work is still valid. Nevertheless, some additional explanation has also been added to the text.

[22] **Please see entire updated section 2.3 for further context and definitions. The specific changes referring to this comment are** [22] **Revision**

Petters [2018] also gives an expression that evaluates to the convolution matrix for passage through a single DMA.

$$\mathbf{A} = \text{mapreduce}\{z^{\mathbf{s}} \rightarrow \Sigma[k \rightarrow T^{\Lambda,\delta}_{size}(k, z^s), m]^T, \text{vcat}, Z\} \tag{11}$$

where, m is the upper number of multiply charged particles, ^{T} is the transpose operator, and Z is a vector of centroid mobilities scanned by the DMA. Eq. (11) evaluates to the same as Eq. (8) in Petters (2018), but the notation is revised to be more general by removing the julia language specific splatting construct and replacing it with the widely used higher-order function mapreduce defined earlier.

To help with parsing the expression, $T^{\Lambda,\delta}_{size}(k, z^s)$ evaluates to a vector of transmission for k charges and set point centroid mobility z^s as a function of the entire mobility grid (e.g. 120 bins discretized between mobility z_1 and z_2). The function $\Sigma[k \rightarrow T^{\Lambda,\delta}_{size}(k, z^s), m]$ superimposes the vectors for all charges. Mapping $z^{\mathbf{s}} \rightarrow \Sigma[k \rightarrow T^{\Lambda,\delta}_{size}(k, z^s), m]$ over the mobility grid Z produces an array of vectors, each corresponding to the transmission for a single size bin. Transposing the vectors and reducing the collection through concatenation produces the design matrix that links the mobility size distribution to the response function, i.e.

$$\mathbb{r} = \mathbf{A}\mathbb{n} + \epsilon \tag{12}$$

where $\mathbb{r}$ is the response distribution, $\mathbb{n}$ is the true mobility size distribution, and ϵ is a vector denoting the random error that may be superimposed as a result of measurement uncertainties. Note that by design $\mathbb{n}$ and $\mathbb{r}$ are *SizeDistribution* objects, which represented the distribution as a histogram in both spectral density units (dN/dlnD) and concentration per bin units.

[23] lines 213, 230: Though z^s is defined in lines 223-224, what is z^s_k in the indicated lines? Since z^s is used in Eq. (10), it might be more conveniently defined in line 211 (rather than line 224) along with Z as "... Z is a vector of centroid mobilities, z^s, scanned by the DMA..." [23] Referee

[24] *The term z^s_k has been rewritten as z^s/k for clarity* [24] *Response*

[25] lines 216-217: "The size distribution after passage through the DMA is given by $\mathbb{r} = \mathbf{A}\mathbb{n} + \epsilon$, where $\mathbb{r}$ is the response function... ." The size distribution exiting the DMA and the response of the detector are not the same thing. The former is usually given as $dN/dlogDp$ while the latter, as in the case of a CPC, is given by N_{CPC}, a simple number concentration. Also, there is the matter of the detector efficiency as well as the transport efficiency between the DMA and the detector, unless the latter has been subsumed into the DMA transport efficiency. As **A** is to later serve as the operator corresponding to transfer through DMA1 in a tandem DMA setup, **A** must represent a size distribution, not a response function. [25] Referee

[26] *It is both. Please see revisions to preceding comment which spells this out. Currently the detector efficiency is not treated separately, but it can be easily added by adding terms to* $T^{\Lambda,\delta}_{size}(k, z^s)$. [26] *Response*

[27] Eq. (11) and following: The double character notation for growth factor as "gf" is atypical as far as normal mathematical notation is concerned. It is too easily interpreted as g times f, rather than as a single parameter. And in this draft of the manuscript there is actually extra space between the two letters, increasing the likelihood of the wrong interpretation. However, it is seen that this space is eliminated in Petters (2018) so presumably it can and will be eliminated in the final typeset form. If not for this preexisting work and a strong preference to remain consistent with that, it would be better to change this to a single character form such as simply "g". Also, the reason for the choice of the cn superscript on $\mathbb{n}^{cn}$ for the input distribution is quite obscure. Does that stand for something? [27] Referee

[28] *The origin for the "cn" superscript was carryover from the previous publication where it was desirable to distinguish the distribution that is measured with a CN counter as detector from a distribution that is measured with a CCN as detector. This way the true activated fraction could be conveniently modeled as* $\mathbb{n}^{ccn}$ *./* $\mathbb{n}^{cn}$. *The "cn" is not needed here and has been dropped; gf has been changed to g for clarity as suggested.* [28] *Response*

[29] line 230: Given the length and complexity of the expression for the operator **O**, it would be better placed on a line by itself and numbered. [29] Referee

[30] *Done* [30] *Response*

[31] **See updated section 2.3** [31] **Revision**

[32] Discretization: As noted (lines 461-462), the forward model for the TDMA rep- [32] Referee

resents a triple integral. The parameters of integration may be denoted as D_i and D_o, the mobility diameters before and after growth, and gf_0, the size-independent growth factor. Though the discretization of these parameters is automated in the software, some discussion of the constraints on this discretization should be included here. For instance, is there a restriction between the number of particle diameter bins and the number of measurement bins? Eq. (15) and the statement (line 248) "The size of $\mathbf{A}_2$ is n^2, ..." would imply that the number of gf bins must be equal to the number of measurement bins. Is this a necessary condition and, if so, why?

[33] *Thank you for raising this. The under-the-hood binning procedure is now explained. The text reflected a choice I made when I wrote the code such that the measurement grid(s) can, but don't have to be interpolated onto any desired grid representation through interpolation (see below). It is worth pointing out here that the generic interface described in section 2.2 is designed such that the user can query the forward model at arbitrary points, which creates non-square matrices that link the grid of P_g and that of DMA 2 measurement representation.* [33] *Response*

[34] **Using the notation in section 2.2,** [34] **Revision**

$$F(\mathrm{x}, \mathrm{c}) = \int_0^\infty P_g \left[\sum_{k=1}^{m} \left(\mathbf{O}_k * \mathbb{M}_k^{\delta_1} \right) \right] dg_0 \tag{17}$$

where x is the true P_g and the vector c of constraining parameters comprises the DMA setup $\Lambda_1, \Lambda_2, \delta_1, \delta_2$ and upstream size distribution $\mathbb{m}$. Computer code that creates a forward model for tandem DMAs has been added to the *DifferentialMobiltyAnalyzers.jl* package and is annotated in the documentation of the package. For purposes of the forward model, the mobility grid for DMA 1 is discretized at a resolution of i bins. Transmission through DMA is computed for a specified z^s (the dry mobility), g_0 (the growth factor), and an input size distribution, which results in a vector i concentrations along this grid. If the input size distribution does not match the mobility grid the grids are merged through interpolation. The mobility grid for DMA 2 is discretized at a resolution of j bins. The transmitted and grown distribution from DMA 1 (i bins along the mobility axis of DMA 1) is interpolated onto the mobility grid of DMA 2. The outer integral in Eq. (17) is discretized into n bins that models P_g. If the output mobility of grid of DMA 2 does not match, the grids are merged through interpolation. The choice of i, j, n, the ranges of mobility grids for DMA 1, DMA 2, and the range of P_g is only constrained by computing resources and a physically reasonable representation of the problem domain. Reasonable choices are $i = 120$, $j = n = 30$. The forward model is used to cast Eq. (17) into matrix form such that the humidified mobility distribution function is given by

$$\mathbb{m}_t^{\delta_2} = \mathbf{A}_2 P_g + \epsilon \tag{18}$$

where the subscript 2 specifies transmission through DMA 2, the matrix $\mathbf{A}_2$ is understood to be computed for a specific input aerosol size distribution, and ϵ is

a vector that denotes the random error that may be superimposed as a result of measurement uncertainties. The size of $\mathbf{A}_2$ is $j \times n$.

[35]Figs. 1-4: Frequency vs. Growth Factor: Growth factor gf and its frequency distribution P_{gf} are naturally continuous functions, though the former is (artificially) discretized for the purposes of inversion. Just as the size distribution, $\mathbb{n}^{cn}$, is explicitly written as dN/dDp or $dN/dlnDp$ with total integral N, the growth factor frequency distribution is also a derivative, dF/dg for $dF/dlngf$, with total integral $F = 1$. However, in the indicated plots, the frequency is plotted as for a parameter with truly discrete values such that the sum of the heights, rather than the areas, of the bars is equal to 1. That is, the height of each bar is given by $(dF/dlngf) \cdot lngf$ where $lngf$ is the width of the bar. If the growth factor is discretized such that lngf is constant, then what is plotted is simply a uniformly scaled version of the more traditional $dF/dlngf$ plot, though this would normally be versus $lngf$. As plotted, the area under these curves is not equal to 1. [35] Referee

[36]Number Concentration vs. Apparent Growth Factor: In these plots, the Apparent Growth Factor is evidently given by
$gf_{app} = D_1(z_2^s)/D_1(z_1^s)$.
The "Concentration"parameter is apparently the first-order inverted number distribution function given by
$dN_{app}/dlnD_{p2} = (dN_{app}/dlnZ_{p2})(dlnZ_p/dlnD_{p2}) = (NCPC/\beta_2)(dlnZ_p/dlnD_{p2})$
where $\beta_2 = Q_{aerosol}/Q_{sheath}$ for DMA 2. This is also seen to be a scaled version of the apparent growth factor frequency distribution as
$dN_{app}/dlnD_{p2} = N_{t,2} \cdot (dF_{app}/dlngf_{app})$
where $N_{t,2}$ is the total concentration exiting DMA 2. If this is to be compared to the Frequency vs. Growth Factor plot, this would need to be multiplied by $lngf_{app} = \Delta lnD_1(z_2^s)$. For the two plots to be directly comparable, $\Delta lnD_1(z_2^s)$ would have to be a constant. [36] Referee

[37]*Combined response to 35 and 36. In the submitted draft, the concentration is the raw number concentration the detector would measure for that bin. Neither the concentration nor the frequency histograms were normalized by the bin width. I changed the revised version to show the probability density functions such that the area under the curve equals to 1. I want to retain the number concentration vs. apparent growth factor plots since the values represent the measurement. I clarify the representation in the text.* [37] *Response*

[38]**Please see revised manuscript.** [38] **Revision**

[39]line 315-316:"...the residual is high ~~is~~ <u>if</u> the true input is a broad growth factor frequency distribution..." [39] Referee

[40]*Fixed* [40] *Response*

[41]lines 332-333: "Errors from scans with low non-zero concentration at the edge of the size distribution propagate back into the inversion at other dry sizes." [41] Referee

[42]*Fixed* [42] *Response*

[43]line 345: "...a cylindrical DMA column (TSI 3080)."Model "3080"does not specify the actual DMA column. Assuming it is the TSI long DMA, this should be specified as either "TSI 3080L"for the whole system or "TSI 3081"for just the column. [43] Referee

[44]*Thank you, we have just the column. Corrected.* [44] *Response*

[45]lines 386-387: "...with the timestamp closest to the ~~a~~ scan..."Eliminate "a" [45] Referee

[46]*Corrected.* [46] *Response*

[47]line 419: "...a marine inflow event on March 27–28 2015."Use a date format consistent with the other dates, i.e. 27-28 March 2015. However, this date is beyond the limits of the plot in Fig. 6. [47] Referee

[48]*The date formats are now consistent. Also, the text should have been 27-28* ***February*** *2015, which is on the plot.* [48] *Response*

[49]line 422: "...9 February 2015,...". Shouldn't this be 11 February 2015? [49] Referee

[50]*Thank you. Corrected.* [50] *Response*

[51]Lines 505-513: "The inverted dataset ...closure (Mahish et al., 2018)." This is a very long run-on sentence. It needs to be broken up into several sentences. [51] Referee

[52]*Done.* [52] *Response*

[53]"Best fit"vs "good fit": Though regularization produces what might be considered a best fit solution to the inversion problem, this does not necessarily imply it is a good fit. It would be best to calculate a fit parameter such as the chi square of the normalized residuals over the degrees of freedom. For a good fit, this should be near 1. That is, the residuals are on the order of what is predicted by Poisson [53] Referee

statistics. Values an order of magnitude or more greater than that would suggest some sort of problem either with the dataset or the model.

[54] *Response*

[54] *It is correct that the best-fit is not necessarily a good fit. Worse, even a good fit may be a poor model. Unregularized regression can almost eliminate the residual, but produce estimation parameters that are extremely poor, even if the regression looks good. For example:*

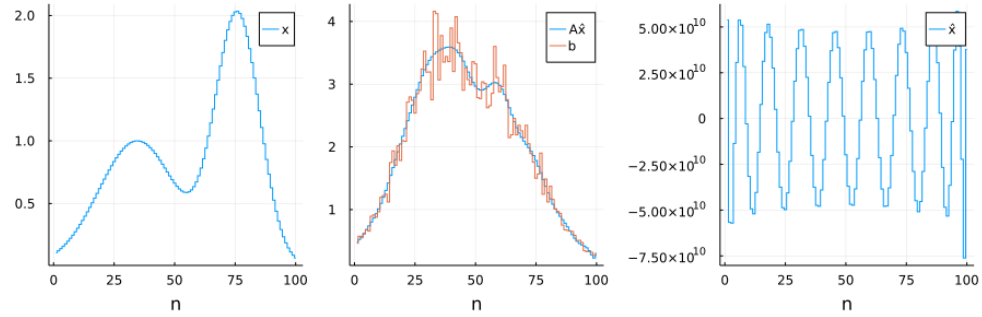

The left panel shows a true input vector x. The middle panel on the left shows a response vector b (red) computed as $\mathrm{b} = \mathbf{A}\mathrm{x} + \epsilon$*, where* ϵ *the some random error. The right panel shows the estimate* $\hat{\mathrm{x}} = \mathbf{A}^{-1}\mathrm{b}$*, which is extremely poor. Computing the model response from the estimate,* $\mathbf{A}\hat{\mathrm{x}}$*, shows the best fit solution. If we only have the observations, we can only compute error metrics based on some residual between* $\mathbf{A}\hat{\mathrm{x}}$ *and* b*. The comment in question in refers to some form of Figure 4*

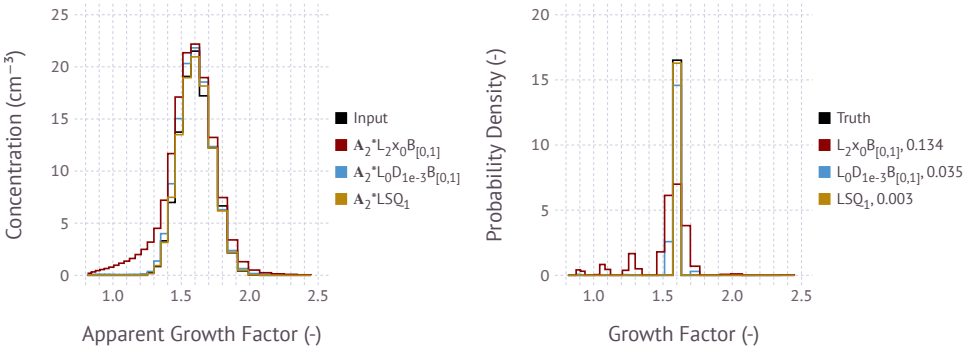

where the left panel corresponds to $\mathbf{A}\hat{\mathrm{x}}$ *(colors) and* b *(Input) in the example above, and the right panel to the comparison between* x *(Truth) and* $\hat{\mathrm{x}}$ *(colors) in the example above. The question raised by this referee (and referee #1) is what the best error metric might be to determine the goodness of the fit and by extension and goodness of model reconstruction. I selected the root mean square error (RMSE),* $RMSE = \sqrt{\sum \frac{(O_i - E_i)^2}{n}}$*, where* O_i *are the observed and* E_i *the expected values. The RMSE is zero for a perfect fit and greater than zero for a less-than optimal fit.*

Many goodness-of-fit statistical tests involve some form of the chi-square statistic. Computing chi-square as $\chi^2 = \sum \frac{(O_i - E_i)^2}{E_i}$*, where* O_i *are the observed and* E_i *the expected values is not valid for many of the cases here, because the expected values can be zero. Any residual in a bin with zero expected value would immediately raise* χ^2 *to infinity. Excluding bins with zero expected value would be incorrect, as it would not capture "bad" models that*

predict output for zero bins. The referee's language "chi square of the normalized residuals over the degrees of freedom" *seems to refer to the adjusted goodness-of-fit index, commonly abbreviated as AGFI [e.g. Sun, 2005], which for the same reason is not valid here.*

The main desired property of a goodness-of-fit index is that it might provide a clean quantitative measure on when to reject a solution. The AGFI seemingly provides this information, with values near 1 indicating a good fit. Although the AGFI is not applicable here, the RMSE can be used in a similar manner. Values below a certain threshold indicate a good (or good enough) fit. The only difference is that the lower threshold value is not immediately clear.

The way RMSE is used here is in a relative comparison between $L_0D_{1e-3}B_{[0,1]}$, LSQ_1, and LSQ_2. LSQ_1, and LSQ_2 are well-behaved and do not have oscillatory solutions. However, they will fail when true growth factor frequency distribution is broader than can be explained by one or two compounds. Conversely $L_0D_{1e-3}B_{[0,1]}$ will have poor solution (oscillatory solution) when the true input distribution is narrow. Truncation of the negative values is what amplifies the RMSE in this case. Thus RMSE is not quite used to declare that the fit is good or that a model is valid. It is used to determine whether the input distribution is narrow enough to warrant fit to a single component, two component, or multicomponent model.

This still leaves the ultimate question unaddressed. How well can we trust the proposed (regularized) solution? As I argue in the manuscript, the simulations address this point.

> Since the true noise-free input growth factor frequency distribution is known, the fidelity of the inversion can be evaluated by computing the root mean square error between the noise-free solution and the regularized solution. The figure shows that both inversion methods produce a root mean square error between 0.02 and 0.03. These values are typical for the of reconstruction (see supporting information). Visual evaluation of the agreement between the reconstruction and the input suggest that either method is suitable for inversion.

Whether this is acceptable remains ultimately up to the user. I am skeptical that a statistical procedure such as AGFI (if it were applicable) would really help here. Tests should be performed to validate the physical plausibility of the solution. For examples, the mode of the apparent growth factor and the mode of the inverted growth factor should be similar. The retrieved growth factors should be physically plausible. The distribution of RMSE can be plotted for a large data set. Visual inspection of fits for large RMSE can be used to derive a threshold above which fits are automatically rejected. The text now mentions these quality assurance examples.

[55] **Note, however, that the low residuals between the apparent growth factor distribution and the model do not automatically ensure that the algorithm a good or adequate solution. Additional tests should be performed to validate the physical plausibility of the solution. For example, the retrieved growth factors should be physically plausible at the applied relative humidity. The mode of the apparent growth factor distribution and the mode of the inverted growth factor distribution should be similar. A histogram of the root mean square error between**

[55] **Revision**

can be plotted for a large data set. Visual inspection of fits for large root mean square error can be used to derive a threshold above which reconstructions are automatically rejected. The integrated probability density function of the reconstructions should be near unity. Deviations from unity may occur due to concentration errors between the size distribution measurement and the growth factor distribution measurement, unaccounted transmission losses, and errors from the inversion. Reconstructions deviating significantly from unity should be flagged and rejected.

Revised Section 2.3

Design Matrices For Differential Mobility Analyzers

Differential mobility analyzers consist of two electrodes held at a constant- or time-varying electric potential. Cylindrical [Knutson and Whitby, 1975] and radial [Zhang et al., 1995, Russell et al., 1996] electrode geometries are the most common. Charged particles in a flow between the electrodes are deflected to an exit slit and measured by a suitable detector, usually a condensation particle counter. The fraction of particles carrying k charges is described by a statistical distribution that is created by the charge conditioner used upstream of the DMA. The functions governing the transfer through bipolar charge conditioners, single DMAs, and tandem DMAs are well understood [Knutson and Whitby, 1975, Rader and McMurry, 1986, Reineking and Porstendörfer, 1986, Wang and Flagan, 1990, Stolzenburg and McMurry, 2008, Jiang et al., 2014].

The traditional mathematical formulation of transfer through the DMA is summarized in Stolzenburg and McMurry [2008] and references therein. Briefly, the integrated response downstream of the DMA operated at voltage V_1 is given by a single integral that includes a summation over all selected charges. The size distribution is measured by varying voltage V_1, which produces the raw response function defined as integrated response downstream of the DMA as a function of upstream voltage. The size distribution is found by inversion. The basic mathematical problem associated with inverting the response function to find the size distribution is summarized by Kandlikar and Ramachandran [1999]. The integral is discretized by quadrature to find the design matrix that maps the size distribution to the response function. L_2 regularization is one of several methods to reconstruct the size distribution from the response function [Voutilainen et al., 2001, Kandlikar and Ramachandran, 1999].

The integrated response downstream of a tandem DMA that is operated at voltages V_1 and V_2 is given by a double integral and the summation of all selected charges. The integrals are over the upstream size distribution and the aerosol conditioner function, which here is the growth factor frequency distribution. Scanning over a range of voltages V_2 results in the raw TDMA response function. The objective is to find find a design matrix that maps the growth factor frequency distribution to the raw TDMA response function.

Petters [2018] introduced a computational approach to model transfer through the DMA. The main idea of the approach is to provide a domain specific language comprising a set of simple building blocks that can be used to algebraically express the response functions intuitively through a form of pseudo code. The main advantage of this approach is that the expressions simultaneously encode the theory governing the transfer through the DMA and the algorithmic solution to compute the response function. The resulting expressions are concise. They are easily identified within actual source code. This makes the code easily modifiable by non-experts to change existing terms or add new convolution terms without the need to develop algorithms.

A disadvantage of the computational approach over the traditional mathematical approach is that computation lacks standardization of notation. This can blur the line between general pseudo code and language specific syntax. Some of the applied computing concepts may be less widely known when compared to standard mathematical approaches. Nevertheless, the author believes that the advantages of the computational approach outweigh the drawbacks. Therefore, this work builds upon the expressions reported in Petters [2018]. Updates and clarifications to the earlier work are noted where appropriate.

The computational language includes a standardized representation of aerosol size distributions, operators to construct expressions, and functions to evaluate the expressions. Size distributions encoded as a *SizeDistribution* composite data type. Composite data types combine multiple arrays into a single symbol for ease of use, facilitating faster experimental design and analysis. *SizeDistribution* consists of vectors of bin edges, bin midpoints, number concentration, log-normalized spectral density, and logarithmic bin widths. *SizeDistributions* are denoted in blackboard bold font (e.g., $\mathbb{n}$, $\mathbb{r}$, etc.). *SizeDistributions* are the building block of composable algebraic expressions through operators that evaluate to transformed *SizeDistributions*. For examples, $\mathbb{n}_1 + \mathbb{n}_2$ is the superposition of two size distributions and $f * \mathbb{n}$ is the uniform scaling of the concentration fields by factor f, $\mathbf{A} * \mathbb{n}$ is matrix multiplication of $\mathbf{A}$ and concentration fields of the size distribution, and $f \cdot \mathbb{n}$ is the uniform scaling of the diameter field of the size distribution by factor f, and $T \cdot \mathbb{n}$ is the elementwise scaling of the diameter field by factor T. (Note that the Petters (2018) used $T. \cdot \mathbb{n}$ is the elementwise scaling. The extra dot has which has been dropped to stay consistent with the current software implementation).

Functions are used to reduce expressions. Generic functions include, $\sum(f, m)$ evaluates the function $f(x)$ for $x = [1, \ldots, m]$ and sums the result. If $f(X)$ evaluates to a vector, the sum is the sum of the vectors. The function map(f, x) applies $f(x)$ to each element of vector x and returns a vector of results in the same order. The function reduce(f, x) applies the bivariate function $f(x, y)$ to each element of x and accumulates the result. The function mapreduce(f, g, x) combines map and reduce. It applies function f to each element in x, and then reduces the result using the bivariate function function $g(x, y)$. The function vcat(x, y) concatenates arrays x and y along one dimension. Anonymous functions are used as arguments to reducing functions. Anonymous functions are denoted as $x \rightarrow expression$, where x is the argument consumed in the evaluation of the $expression$. These functions are generic and represent widely used computing concepts. They are implemented in most modern programming languages.

DMA geometry, dimensions, and configuration are abstracted into composite types Λ (configuration comprising flow rates, power supply polarity, and thermodynamic state) and δ (DMA domain defined by a mobility/size grid). Each DMA is fully described by a pair Λ,δ. Subscripts and superscripts are used to distinguish between different configurations in chained DMA setups, e.g. δ_1 and δ_2 denoting the first and second DMA, respectively. Application of size distribution expressions to transfer functions constructs a concise model of the transmitted DMA mobility distribution, denoted as the DMA response function. Implementation of the language is distributed through a freely-available and independently documented package *DifferentialMobilityAnalyzers.jl*, written in the Julia language. Expressions in the text are provided in general mathematical form for readability.

Petters [2018] gives a simple expressions that model transfer through the DMA. The function $T_{size}^{\Lambda,\delta}(k, z^s)$ evaluates to a vector representing the fraction of particles carrying k charges that exit DMA$^{\Lambda,\delta}$ as a function of mobility

$$T_{size}^{\Lambda,\delta}(k, z^s) = \Omega(Z, z^s/k, k). * T_c(k, D_{p,1}). * T_l(Z, k) \tag{10}$$

where z^s is the centroid mobility selected by the DMA (determined by the voltage and DMA geometry), Z is a vector of mobilities, Ω is the diffusing DMA transfer function [Stolzenburg and McMurry, 2008], T_c is the charge frequency distribution [Wiedensohler, 1988], and T_l is the diameter-dependent transmission loss [Reineking and Porstendörfer, 1986]. The functions Ω and

T_l have been updated from Petters (2018). The version in Petters (2018) computed the shape of the transfer function and losses for the mobility diameter corresponding to singly charged particles and then apply the same shape of the transfer function and diffusional loss to the multiply charged particles. Binding the charge state explicitly to Ω and T_l results in proper accounting of diffusional losses and broadening of the transfer function for multiply charged particles in $T_{size}^{\Lambda,\delta}(k, z^s)$.

Petters [2018] also gives an expression that evaluates to the convolution matrix for passage through a single DMA.

$$\mathbf{A} = \text{mapreduce}\{z^s \rightarrow \Sigma[k \rightarrow T_{size}^{\Lambda,\delta}(k, z^s), m]^T, \text{vcat}, Z\} \tag{11}$$

where, m is the upper number of multiply charged particles, ^{T} is the transpose operator, and Z is a vector of centroid mobilities scanned by the DMA. Eq. (11) evaluates to the same as Eq. (8) in Petters (2018), but the notation is revised to be more general by removing the julia specific splatting construct and replacing it with widely used generic functions.

To help with parsing the expression, $T_{size}^{\Lambda,\delta}(k, z^s)$ evaluates to a vector of transmission for k charges and set point centroid mobility z^s as a function of the entire mobility grid (e.g. 120 bins discretized between mobility z_1 and z_2). The function $\Sigma[k \rightarrow T_{size}^{\Lambda,\delta}(k, z^s), m]$ superimposes the vectors for all charges. Mapping $z^s \rightarrow \Sigma[k \rightarrow T_{size}^{\Lambda,\delta}(k, z^s), m]$ over the mobility grid Z produces an array of vectors, each corresponding to the transmission for a single size bin. Transposing the vectors and reducing the collection through concatenation produces the design matrix that links the mobility size distribution to the response function, i.e.

$$\mathbb{r} = \mathbf{A}\mathbb{n} + \epsilon \tag{12}$$

where $\mathbb{r}$ is the response distribution, $\mathbb{n}$ is the true mobility size distribution, and ϵ is a vector denoting the random error that may be superimposed as a result of measurement uncertainties. Note that by design $\mathbb{n}$ and $\mathbb{r}$ are *SizeDistribution* objects, which represented the distribution as a histogram in both spectral density units (dN/dlnD) and concentration per bin units. The latter is the raw response function defined as integrated response downstream of the DMA as a function of upstream voltage (or corresponding z^s or corresponding apparent +1 mobility diameter).

The mobility distribution exiting DMA 2 in the humidified tandem DMA is evaluated using the expressions

$$\mathbb{M}_k^{\delta_1} = \Pi_k \cdot \left\{ g_0 \cdot \left[T_{size}^{\Lambda,\delta}(k, z^s) * \mathbb{n} \right] \right\} \tag{13}$$

In Eq. (13), $\mathbb{M}_k^{\delta_1}$ evaluates to the apparent +1 mobility distribution particles that exit the DMA$^{\Lambda,\delta}$ at the nominal setpoint-diameter defined by mobility z^s (or z-star) in DMA 1 and particle charge k. Subscripts are used to differentiate DMA 1 and 2 which possibly have different geometries, flow rates, and grids, e.g. Λ_1, Λ_2 and δ_1, δ_2. $\Pi_k^{\Lambda,\delta}$ is the projection of particles having physical diameter D and carrying k charges onto the apparent +1 mobility grid. It is a function that converts each diameter/charge pair to mobility and interprets the result as apparent +1 mobility diameter. $g_0 = D_{wet}/D_{dry}$ is the true diameter growth factor, D_{dry} is the selected diameter by DMA 1, D_{wet} is the diameter after the humidifier, $T_{size}^{\Lambda,\delta}(k, z^s)$ is as in Eq. (10), and $\mathbb{n}$ is the mobility size distribution upstream of DMA 1.

To help parse Eq. (13), the product $T_{size}^{\Lambda,\delta}(k, z^s) * \mathbb{n}$ evaluates to the transmitted mobility distributions of particles carrying k charges at the set-point mobility z^s in DMA 1. The size distribution is

grown by the growth factor g_0. The resulting size distribution is shifted to the apparent +1 mobility diameter using $\Pi_k^{\Lambda,\delta}$. Equation (13) differs from that in Petters [2018] where it was assumed that particles of all charges grow by the same amount. This is incorrect. Particles carrying more than a single charge alias at a smaller particle size [Gysel et al., 2009, Shen et al., 2021]. The effect is due to the size dependence of the slip-flow correction factor and captured through the function $\Pi_k^{\Lambda,\delta}$. Equation (13) assumes that g_0 applies to all particle sizes.

The total humidified mobility distribution $\mathbb{m}_t^{\delta_2}$ exiting DMA 2 is given by

$$\mathbb{m}_t^{\delta_2} = \sum_{k=1}^{m} \left(\mathbf{O}_k * \mathbb{M}_k^{\delta_1} \right) \tag{14}$$

where, m is upper number of charges on the multiply charged particles, Z is a vector of centroid mobilities scanned by DMA 2, and

$$\mathbf{O}_k = \text{mapreduce}\{z^s \rightarrow [\Omega^{\Lambda_2,\delta_2}(Z, z^s, k). * T_l^{\Lambda_2,\delta_2}(Z, k)]^T, \text{vcat}, Z\} \tag{15}$$

is the convolution matrix for transport through DMA 2 and particles carrying k charges. Equations (14) and (15) modified from those in Petters (2018) in the following manner. The convolution matrix $\mathbf{O}_k$ is computed individually for each charge. The version in Petters (2018) computed the matrix corresponding to singly charged particles and then apply the same matrix to multiply charged particles. Since $\mathbf{O}_k$ is now charge resolved, it is moved into the summation in Eq. (14). Computation of $\mathbf{O}_k$ through Eq. (15) has been revised to be more general by removing a julia language specific construct. $\mathbf{O}_1$ computed by Eq. (15) produces the same matrix as in Petters (2018).

If the aerosol is externally mixed, the humidified distribution function is given by

$$\mathbb{m}_t^{\delta_2} = \int_0^\infty P_g \left[\sum_{k=1}^{m} \left(\mathbf{O}_k * \mathbb{M}_k^{\delta_1} \right) \right] dg_0 \tag{16}$$

where P_g is the growth factor probability density function and the diameters in $\mathbb{M}_k^{\delta_1}$ are normalized by D_{dry}. $\mathbb{m}_t^{\delta_2}$ in Eq. (16) is the forward model through the tandem DMA. Using the notation in section 2.2,

$$F(\mathrm{x}, \mathrm{c}) = \int_0^\infty P_g \left[\sum_{k=1}^{m} \left(\mathbf{O}_k * \mathbb{M}_k^{\delta_1} \right) \right] dg_0 \tag{17}$$

where x is the true P_g and the vector c of constraining parameters comprises the DMA setup $\Lambda_1, \Lambda_2, \delta_1, \delta_2$ and upstream size distribution $\mathbb{n}$. Computer code that creates a forward model for tandem DMAs has been added to the *DifferentialMobiltyAnalyzers.jl* package and is annotated in the documentation of the package. For purposes of the forward model, the mobility grid for DMA 1 is discretized at a resolution of i bins. Transmission through DMA is computed for a specified z^s (the dry mobility), g_0 (the growth factor), and an input size distribution, which results in a vector i concentrations along this grid. If the input size distribution does not match the mobility grid the grids are merged through interpolation. The mobility grid for DMA 2 is discretized at a resolution of j bins. The transmitted and grown distribution from DMA 1 (i bins along the mobility axis of DMA 1) is interpolated onto the mobility grid of DMA 2. The outer integral in Eq. (17) is discretized into n bins that models P_g. If the output mobility of grid of DMA 2 does not match, the grids are merged through interpolation. The choice of i, j, n, the ranges of mobility grids for DMA 1, DMA 2, and the range of P_g is only constrained by computing resources and a physically

reasonable representation of the problem domain. Reasonable choices are $i = 120$, $j = n = 30$. The forward model is used to cast Eq. (17) into matrix form such that the humidified mobility distribution function is given by

$$\mathrm{m}_t^{\delta_2} = \mathbf{A}_2 P_g + \epsilon \tag{18}$$

where the subscript 2 specifies transmission through DMA 2, the matrix $\mathbf{A}_2$ is understood to be computed for a specific input aerosol size distribution, and ϵ is a vector that denotes the random error that may be superimposed as a result of measurement uncertainties. The size of $\mathbf{A}_2$ is $j \times n$. Uncertainties in the size distribution propagate into $\mathbf{A}_2$. The main influence of the error will be the relative fraction of +1, +2, and +3 charged particles. Assuming a random error of $\pm 20\%$ in concentration, the overall effect on the $\mathrm{m}_t^{\delta_2}$ is expected to small.

References

M. Gysel, G.B. McFiggans, and H. Coe. Inversion of tandem differential mobility analyser (TDMA) measurements. *Journal of Aerosol Science*, 40(2):134–151, February 2009. ISSN 0021-8502. DOI: 10.1016/j.jaerosci.2008.07.013.

Jingkun Jiang, Chungman Kim, Xiaoliang Wang, Mark R. Stolzenburg, Stanley L. Kaufman, Chaolong Qi, Gilmore J. Sem, Hiromu Sakurai, Naoya Hama, and Peter H. McMurry. Aerosol Charge Fractions Downstream of Six Bipolar Chargers: Effects of Ion Source, Source Activity, and Flowrate. *Aerosol Science and Technology*, 48(12):1207–1216, December 2014. ISSN 0278-6826. DOI: 10.1080/02786826.2014.976333.

Milind Kandlikar and Gurumurthy Ramachandran. Inverse Methods for Analysing Aerosol Spectrometer Measurements: A Critical Review. *Journal of Aerosol Science*, 30(4):413–437, 1999. ISSN 0021-8502. DOI: 10.1016/S0021-8502(98)00066-4.

E. O. Knutson and K. T. Whitby. Aerosol classification by electric mobility: Apparatus, theory, and applications. *Journal of Aerosol Science*, 6(6):443–451, 1975. ISSN 0021-8502. DOI: 10.1016/0021-8502(75)90060-9.

M. D. Petters. A language to simplify computation of differential mobility analyzer response functions. *Aerosol Science and Technology*, 52(12):1437–1451, December 2018. ISSN 0278-6826. DOI: 10.1080/02786826.2018.1530724.

D.J. Rader and P.H. McMurry. Application of the tandem differential mobility analyzer to studies of droplet growth or evaporation. *Journal of Aerosol Science*, 17(5):771–787, January 1986. ISSN 0021-8502. DOI: 10.1016/0021-8502(86)90031-5.

A. Reineking and J. Porstendörfer. Measurements of Particle Loss Functions in a Differential Mobility Analyzer (TSI, Model 3071) for Different Flow Rates. *Aerosol Science and Technology*, 5(4): 483–486, January 1986. ISSN 0278-6826. DOI: 10.1080/02786828608959112.

Lynn M. Russell, Shou-Hua Zhang, Richard C. Flagan, John H. Seinfeld, Mark R. Stolzenburg, and Robert Caldow. Radially Classified Aerosol Detector for Aircraft-Based Submicron Aerosol Measurements. *Journal of Atmospheric and Oceanic Technology*, 13(3):598–609, June 1996. ISSN 0739-0572. DOI: 10.1175/1520-0426(1996)013<0598:RCADFA>2.0.CO;2.

C. Shen, G. Zhao, and C. Zhao. Effects of multi-charge on aerosol hygroscopicity measurement by a HTDMA. *Atmospheric Measurement Techniques*, 14(2):1293–1301, 2021. DOI: 10.5194/amt-14-1293-2021.

Mark R. Stolzenburg and Peter H. McMurry. Equations Governing Single and Tandem DMA Configurations and a New Lognormal Approximation to the Transfer Function. *Aerosol Science and Technology*, 42(6):421–432, April 2008. ISSN 0278-6826. DOI: 10.1080/02786820802157823.

Jun Sun. Assessing Goodness of Fit in Confirmatory Factor Analysis. *Measurement and Evaluation in Counseling and Development*, 37(4):240–256, January 2005. ISSN 07481756. DOI: 10.1080/07481756.2005.11909764.

A. Voutilainen, V. Kolehmainen, and J. P. Kaipio. Statistical inversion of aerosol size measurement data. *Inverse Problems in Engineering*, 9(1):67–94, January 2001. ISSN 1068-2767. DOI: 10.1080/1741597010880277753.

Shih Chen Wang and Richard C. Flagan. Scanning Electrical Mobility Spectrometer. *Aerosol Science and Technology*, 13(2):230–240, January 1990. ISSN 0278-6826. DOI: 10.1080/02786829008959441.

A. Wiedensohler. An approximation of the bipolar charge distribution for particles in the submicron size range. *Journal of Aerosol Science*, 19(3):387–389, June 1988. ISSN 0021-8502. DOI: 10.1016/0021-8502(88)90278-9.

Shou-Hua Zhang, Yoshiaki Akutsu, Lynn M. Russell, Richard C. Flagan, and John H. Seinfeld. Radial Differential Mobility Analyzer. *Aerosol Science and Technology*, 23(3):357–372, January 1995. ISSN 0278-6826. DOI: 10.1080/02786829508965320.